AIP | Review of Scientific Instruments

Note: Diagnosing femtosecond laser-solid interactions with monochromatic K α imager and x-ray pinhole camera

X. X. Lin, Y. T. Li, F. Liu, B. C. Liu, F. Du, S. J. Wang, L. M. Chen, L. Zhang, Y. Zheng, X. Liu, X. L. Liu, Z. H. Wang, J. L. Ma, Z. Y. Wei, and J. Zhang

Citation: Review of Scientific Instruments **82**, 036104 (2011); doi: 10.1063/1.3567014
View online: http://dx.doi.org/10.1063/1.3567014
View Table of Contents: http://scitation.aip.org/content/aip/journal/rsi/82/3?ver=pdfcov
Published by the AIP Publishing

Note: Diagnosing femtosecond laser-solid interactions with monochromatic K_α imager and x-ray pinhole camera

X. X. Lin (林晓宣),[1] Y. T. Li (李玉同),[1,a)] F. Liu (刘峰),[1] B. C. Liu (刘必成),[1,2,3]
F. Du (杜飞),[1] S. J. Wang (王首钧),[1] L. M. Chen (陈黎明),[1] L. Zhang (张璐),[1]
Y. Zheng (郑轶),[1] X. Liu (刘勋),[1] X. L. Liu (刘晓龙),[1] Z. H. Wang (王兆华),[1]
J. L. Ma (马景龙),[1] Z. Y. Wei (魏志义),[1] and J. Zhang (张杰)[1,4,b)]
[1]*Beijing National Laboratory for Condensed Matter Physics, Institute of Physics, Chinese Academy of Sciences, Beijing 100190, China*
[2]*State Key Laboratory of Nuclear Physics and Technology, Peking University, Beijing 100871, China*
[3]*Graduate University of the Chinese Academy of Sciences, Beijing 100049, China*
[4]*Shanghai Jiao Tong University, Shanghai 200240, China*

(Received 1 November 2010; accepted 21 February 2011; published online 23 March 2011)

An x-ray pinhole camera and a monochromatic K_α imager are used to measure the interactions of intense femtosecond laser pulses with Cu foil targets. The two diagnostics give different features in the spot size and the laser energy scaling, which are resulted from different physical processes. Under our experimental conditons, the K_α emission is mainly excited by the fast electrons transporting inside the cold bulk target. In contrast, the x-ray pinhole signals are dominated by the broadband thermal x-ray emission from the hot plasma at the front target surface. © *2011 American Institute of Physics*. [doi:10.1063/1.3567014]

X-ray pinhole camera[1] and K_α imager[2] are two kinds of widely used two-dimensional (2D) x-ray imaging techniques. The x-ray emission detected by a pinhole camera is a mixture of broadband and line emission from various excitation mechanisms, and its energy range is determined by the filter and the detector. Recently, the K_α imager is used to characterize fast electron transport inside the target by measuring the K_α line emission excited by the fast electrons.[3] Since both the broadband and line emission can be emitted from the hot plasma and the cold bulk target region, the comparison of x-ray pinhole and K_α imaging measurements is helpful to investigate the corresponding physical processes revealed by the two diagnostics.

In this paper, the measurements of x-ray pinhole and K_α imaging are comparatively studied. Their spot sizes are both larger than the laser focal spot, and the K_α spot is the largest. The integral x-ray pinhole signal and the K_α yield show obviously different trends as the laser energy increases. It is found that, under the typical femtosecond laser-produced plasma conditions, the K_α imager mainly reveals the fast electron transport in the bulk target, and the x-ray pinhole signals are originated mainly from the broadband thermal x-ray emission excited in hot plasma.

The experiments were carried out using the Xtreme light (XL) II Ti: sapphire laser system at the Institute of Physics, Chinese Academy of Sciences, which can deliver a laser pulse with energy up to 0.6 J in 60 fs at 800 nm.[4] The p-polarized laser pulse was focused onto a 50 μm thick Cu foil target at an incidence angle of 45° with an *f*/3.5 off-axis parabolic mirror. The diameter of the focal spot was ~4.5 μm at the full width at half maximum, which contained ~35% of the laser energy. The laser intensity was up to 5×10^{18} W/cm^2.

An x-ray pinhole camera equipped with a 16 bit charge-coupled device (CCD) (PI-SX) was mounted to view the front target surface at an angle of 60° with respect to the target normal. The pinhole diameter was ~20 μm and the magnification was ~10. The spatial resolution was ~22 μm.[1] A 1.2 μm thick Al filter was put in front of the pinhole. The photon energy range detected by the pinhole camera was mainly from 0.4 to 10 keV.

A spherically bent quartz 2131 crystal was used to image the Cu K_α emission at 8.048 keV onto a 16 bit CCD (Andor-DO434BN) with a magnification of ~8. A 30 mm diameter aperture was put in front of the crystal, giving an astigmatism-limited spatial resolution of ~19 μm.[2] The energy bandwidth was about 11 eV.[5] The crystal viewed the front target surface at an angle of 48° with respect to the target normal. The K_α yield was measured with a single photon counting CCD (PI-LCX) which also viewed the front target surface.

Figure 1 shows the typical images of the laser focal spot, x-ray pinhole spot, and K_α emission spot. The laser focal spot is measured with the attenuated full laser energy. The pinhole spot and the K_α spot are measured with a laser energy of ~150 mJ. The spot sizes are much different. The FWHM of these three spots are 4.5, 35, and 85 μm, respectively.

Figure 2 shows the integral pinhole signal intensities and the K_α yield measured by the single photon counting CCD. The K_α yield increases linearly as the laser energy increases from 50 to 190 mJ, and then becomes saturated. We also checked the calibrated integral intensities of the images measured by the K_α crystal imager, which show the similar trend. Although the K_α emission from the hot plasma may also contribute to the signals of the K_α imager, it is found that this contribution can be ignored under our experimental conditions. Because the integral intensities of the K_α images with a narrow detection range do not show any decrease than the single photon counting CCD signals at high laser energy, and these

a)Electronic mail: ytli@aphy.iphy.ac.cn.
b)Electronic mail: jzhang@aphy.iphy.ac.cn.

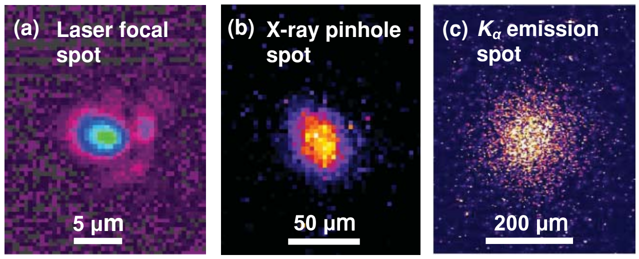

FIG. 1. (Color online) Typical images of (a) laser focal spot, (b) x-ray pinhole spot, and (c) K_α spot.

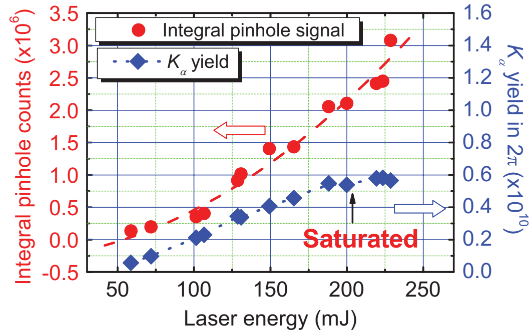

FIG. 2. (Color online) The integral x-ray pinhole signal intensity (red circle) and the K_α yield in 2π steradian (blue diamond) as a function of laser energy.

two K_α diagnostics show the similar trend as the laser energy increases, when the broadening and shifting of the K-shell radiation will occur.[5] Thus, the K_α image mainly reveals the K_α emission from the cold target. The saturation of the K_α yield at high laser intensity has also been observed previously.[3] The fast electron temperature exceeding the optimal value for the K-shell ionization cross section[6] and the enhanced reabsorption of the photons inside deeper region of the target, at high laser energy, can lead to the saturation of the K_α yield.[3]

In contrast, the integral pinhole signal intensities shown in Fig. 2 continually increase with the laser energy and no saturation appears. Because of the wide energy range detected by the pinhole camera, both continuum and K-shell emission, excited inside the cold bulk target, contribute to the pinhole signals. Another origin is the thermal broadband x-ray emission from the hot plasma at the front target surface.

The Monte Carlo code MCNP4C is used to estimate the continuum and K-shell emission excited inside the *cold bulk* target. Considering the experimental setup and the response curve of the detectors, the K_α yield in 2π steradians and the integrated pinhole counts are calculated. In the calculation, the fast electrons, assumed to be Maxwellian distributed, are normally injected into a 50 μm thick planar Cu target, and the fast electron temperature $T_{\rm hot}$ is related to the laser energy by Wilks's scaling.[7] The total number of the fast electrons N_e is estimated as $N_e \sim \varepsilon_{\rm L}\eta_{\rm L\text{-}e}/{\rm T_{hot}}$, where ε_L is the laser energy and $\eta_{L\text{-}e}$ is the conversion efficiency of laser energy into fast electrons.

Since $\eta_{L\text{-}e}$ is a function of the laser intensity,[8] it is assumed to be 1 in the MC calculations first. Then the real $\eta_{L\text{-}e}$ at a specific ε_L is estimated with the ratio of the measured K_α yield to the MC calculated result. Figure 3(a) shows the MC calculated K_α yield (with $\eta_{L\text{-}e} = 1$) and the experimental data. The inset shows the inferred $\eta_{L\text{-}e}$, which increases from 3% to 26% as the laser energy increases from 50 to 230 mJ. This is consistent with the previous result.[8]

Figure 3(b) shows the MC calculated integral x-ray emission for the pinhole camera due to the continuum and line emission excited inside the cold bulk target, when $\eta_{L\text{-}e}$ is set to be 1. Even with $\eta_{L\text{-}e} = 1$, the MC result is less by almost two orders than the experimental data. This indicates that the bremsstrahlung and K-shell emission, excited inside the cold bulk target, may be not the main contribution to the x-ray pinhole signals, for our experimental conditions.

To investigate the contribution of the broadband x-ray emission and the K-shell emission from the hot plasma and the cold bulk target, FLYCHK[9] with a non local thermodynamic equilibrium model is used. For simplification, the characteristic average electron density n_e for the hot Cu plasma and the cold bulk Cu target are set to be 10^{21} cm^{-3} and 10^{23} cm^{-3}, respectively. The electron temperature T_e is varied from 10 to 500 eV for the hot plasma, and from 1 to 50 eV for the cold bulk target. The typical fast electron temperature $T_{\rm hot}$ is set to be 300 keV.[7] The results are shown in Fig. 4. It can be seen that, for $T_e = 10$ eV, which is typically low for the hot plasma but high for cold bulk, the integral K-shell emission from the hot plasma is still less by almost two orders than that from cold bulk. Thus for the hot plasma with $T_e \geq 10$ eV, and the bulk target with $T_e \leq 10$ eV, the K-shell emission is mainly excited by the fast electrons in the cold bulk target. Furthermore, as T_e increases, strong thermal x-ray less than

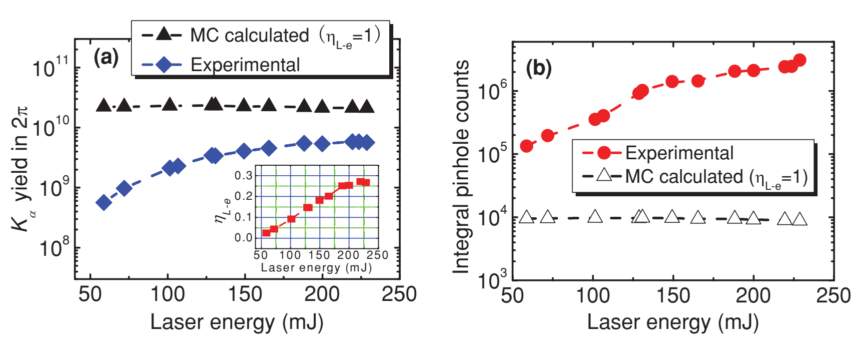

FIG. 3. (Color online) (a) The MC calculated K_α yield taking $\eta_{L\text{-}e} = 1$ (black solid triangle) and the measured K_α yield (blue diamond). The inset shows the inferred conversion efficiencies of the laser energy into fast electrons. (b) The MC calculated integral x-ray emission for the pinhole camera (open triangle) and the experimental data (red circle).

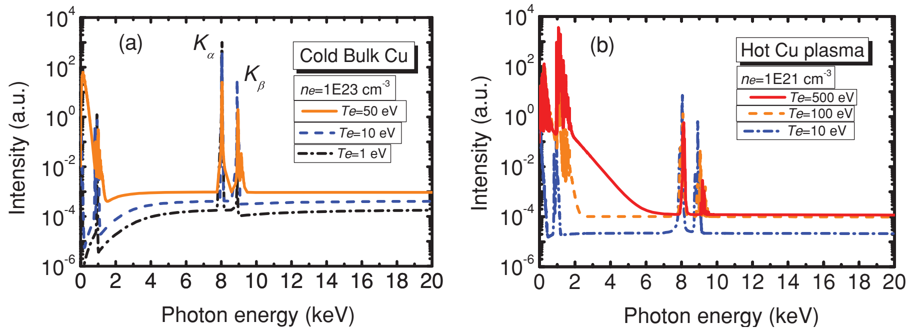

FIG. 4. (Color online) The FLYCHK calculated x-ray emission spectra from (a) the cold Cu bulk ($n_e = 10^{23}$ cm^{-3}) and (b) the hot Cu plasma ($n_e = 10^{21}$ cm^{-3}), with varied electron temperatures, both taking 300 keV fast electrons into account.

5 keV with a peak around 1.2 keV can be excited. It is found that, for the hot plasma with $T_e \geq 50$ eV and the cold bulk target with $T_e \leq 10$ eV, the broadband emission corresponding to the pinhole detection range, from the bulk target is less by two orders than that from the hot plasma. Therefore, for such conditions, the x-ray pinhole image mainly reveals the hot plasma region.

Taking into account the possible contribution of the thermal x-ray emission from the hot plasma to the pinhole signals in our experimental conditions, the observations can be explained. The hot plasma lateral expansion during and after the laser irradiation leads to a larger time-integrated pinhole spot than the laser focal spot. In contrast, the K_α emission is mainly excited by the fast electrons which can be significantly influenced by the self-generated fields and transport long distance inside the target, leading to an enhanced lateral electron transport.[10] Therefore, the K_α spot can be much larger than the hot plasma region revealed by the pinhole spot. In addition, the positive dependence of the hot plasma x-ray emission on the laser energy can cause the continuous increase of the pinhole signals in Fig. 2.

In summary, we have comparatively studied the measurements of x-ray pinhole camera and K_α imager. It indicates that, for the typical range of conditions of the relativistic femtosecond laser-produced plasmas, the K_α imaging technique is suitable for the diagnostic of fast electron transport, and the x-ray pinhole camera can reveals the hot plasma region. Different imaging diagnostics should be carefully chosen to estimate different physical parameters, such as laser intensity, hot plasma size, and fast electron transport region.

This work is supported by the National Nature Science Foundation of China (Grant Nos. 10925421, 10735050, 10974250, 10935002), National Basic Research Program of China (973 Program) (Grant No. 2007CB815101) and the National High-Tech ICF program.

[1] D. B. Sinars, G. R. Bennett, D. F. Wenger, M. E. Cuneo, and J. L. Porter, Appl. Opt. **42**, 4059 (2003).
[2] J. A. Koch, Y. Aglitskiy, C. Brown, T. Cowan, R. Freeman, S. Hatchett, G. Holland, M. Key, A. MacKinnon, J. Seely, R. Snavely, and R. Stephens, Rev. Sci. Instrum. **74**, 2130 (2003).
[3] C. Reich, P. Gibbon, I. Uschmann, and E. Forster, Phys. Rev. Lett. **84**, 4846 (2000).
[4] J. Zhang, Y. T. Li, Z. M. Sheng, Z. Y. Wei, Q. L. Dong, and X. Lu, Appl. Phys. B **80**, 957 (2005).
[5] K. U. Akli, M. H. Key, H. K. Chung, S. B. Hansen, R. R. Freeman, M. H. Chen, G. Gregori, S. Hatchett, D. Hey, N. Izumi, J. King, J. Kuba, P. Norreys, A. J. MacKinnon, C. D. Murphy, R. Snavely, R. B. Stephens, C. Stoeckel, W. Theobald, and B. Zhang, Phys. Plasmas **14**, 023102 (2007).
[6] C. A. Quarles, Phys. Rev. A **13**, 1278 (1975).
[7] S. C. Wilks, W. L. Kruer, M. Tabak, and A. B. Langdon, Phys. Rev. Lett. **69**, 1383 (1992).
[8] R. R. Freeman, D. Batani, S. Baton, M. Key, and R. Stephens, Fusion Sci. Technol. **49**, 297 (2006)
[9] H. K. Chung, M. H. Chen, W. L. Morgan, Y. Ralchenko, and R. W. Lee, High Energy Density Phys. **1**, 3 (2005).
[10] Y. T. Li, X. H. Yuan, M. H. Xu, Z. Y. Zheng, Z. M. Sheng, M. Chen, Y. Y. Ma, W. X. Liang, Q. Z. Yu, Y. Zhang, F. Liu, Z. H. Wang, Z. Y. Wei, W. Zhao, Z. Jin, and J. Zhang, Phys. Rev. Lett. **96**, 165003 (2006).